Synthesis and pH-Dependent Spectroscopic Behavior of 2,4,6-Trisubstituted Pyridine Derivatives

Gala Chapman,[a] Isaac Solomon,[a] Gabor Patonay,[a]* and Maged Henary[a]*

Department of Chemistry, Georgia State University, P.O. Box 4098, Atlanta, Georgia 30302-4098
*E-mail: gpatonay@gsu.edu; mhenary1@gsu.edu

Additional Supporting Information may be found in the online version of this article.
Received August 25, 2012
DOI 10.1002/jhet.1923
Published online 00 Month 2014 in Wiley Online Library (wileyonlinelibrary.com).

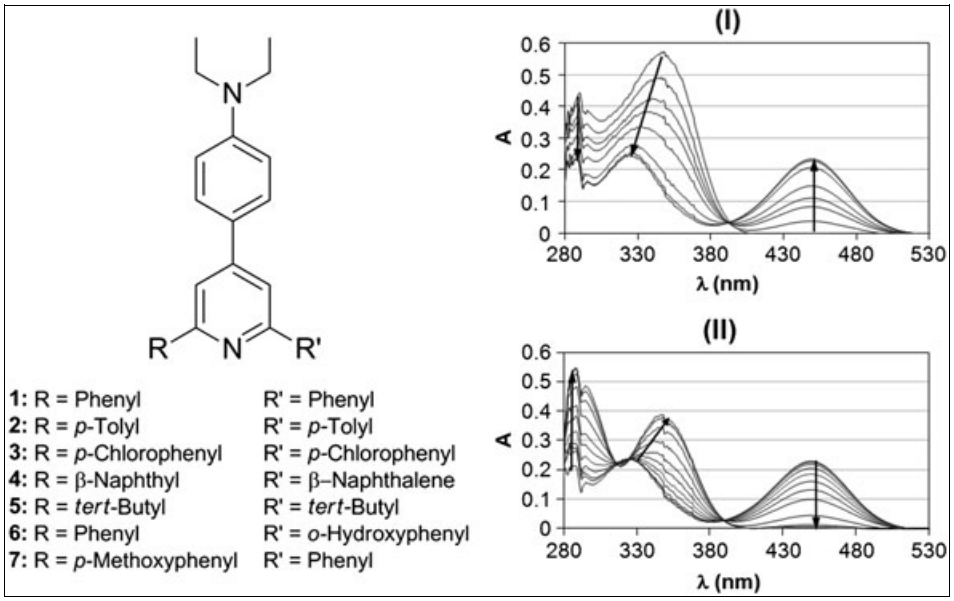

Seven 2,4,6-trisubstituted pyridine derivatives with *N*,*N*-diethylaniline substituents at the 4-position were synthesized, and their spectroscopic properties in the absence and presence of acid were studied. The spectral effects of protonation, molar absorptivities, pK_a values, and the structural origins of the observed spectral behavior were ascertained. The pyridine nitrogen was found to be more basic than the diethylamino nitrogen atom. Protonation of the pyridine ring nitrogen is associated with the appearance of a red-shifted intramolecular charge transfer peak in the UV-visible spectra. Favorable color indicating properties result from electron-donating substitution at the 2 and 6 positions of pyridine, which provide a greater absorptivity of the red-shifted peak associated with protonation of the pyridine nitrogen. These findings will assist in the design and optimization of these compounds for ion-indicating and pH-sensing applications.

INTRODUCTION

Pyridine derivatives substituted at the 2, 4, and 6 positions have a wide variety of applications, most of which are based upon their photophysical properties. Applications of these compounds include thermal recording materials [1], photographic acid-mediated imaging media [2], photocurable compositions for stereolithography, tunable dye lasers [3], and ion probes [4,5].

Pyridines conjugated to a heteroatom with electron-donating resonance effects can be classified as a type of merocyanine dye, which are of particular interest due to their solvatochromic properties. Betaine dyes possessing a 2,4,6-trisubstituted pyridinium moiety linked to a phenolate group exhibit dramatic solvatochromic effects [6] and thermochromic properties [7]; thus, these compounds have potential applications in thermochromic media. These properties are the result of a pronounced difference in dipole moment between the ground and excited states of the molecule because of an intramolecular charge transfer (ICT) between the donor and acceptor groups [6]. These charge transfer properties give rise to a long wavelength ICT band in the absorption spectrum because of the $\pi \rightarrow \pi^*$ transition [6].

Substituents at the 2, 4, and 6 positions can act as donor groups to the pyridine nitrogen because of their *ortho* or *para* orientation; accordingly, they are potential modulators of the spectroscopic properties of these compounds. When a donor group is also nucleophilic, binding of cations can either occur at the donor group or the acceptor pyridine group. To model and evaluate the effects of substitution on the spectroscopic properties of such ditopic compounds, spectral data can be collected both for the compounds alone and in the presence of a protonating agent or an appropriate metal ion. However, by using an acid instead of a metal ion, the spectral behavior

corresponding to binding at each of the nucleophilic sites can be modeled separately by simply changing the concentration of a single acidic species rather than using different metals with specific affinities for different nucleophilic sites. Moreover, this approach circumvents the possibility of partial conjugation at both of the nucleophilic sites by metal ions with mixed affinities; hence, such protonation studies provide a picture that is easier to interpret regarding the spectral and physical changes in the unknown upon ion binding.

The primary purpose of our study was to synthesize ditopic 2,4,6-trisubstituted pyridine derivatives with *para-N*, *N*-diethylaniline substitution at the 4 position and varying substitution at the 2 and 6 positions and to determine the effect of varying substitution on the UV-visible spectroscopic behavior in various solvents in the presence of various acids. To date, limited data is available on the changes to the photophysical characteristics associated with varying the substitution at the 2 and 6 positions of these compounds. Protonation studies were carried out, and molar absorptivities of peaks corresponding to the basic and singly protonated forms of the compounds were determined. For selected compounds, acid dissociation constants were determined spectroscopically, and molar absorptivities of the nonprotonated and singly protonated forms were determined in different solvent systems using different acids to determine the effects of solvent and acid strength on the photophysical behavior. Finally, a correlated NMR-absorption study was carried out on one of the compounds to experimentally verify the order of protonation of the basic nitrogen atoms. Similar NMR studies were also carried out at higher and lower temperature to ensure that the order of protonation is not temperature dependent. These studies to determine the effects of changing substitution at the 2 and 6 positions, and the effects of solvents and acid strength will assist targeted design of these compounds for their myriad of applications, particularly as ion probes and pH sensors.

RESULTS AND DISCUSSION

Synthesis. Symmetrically substituted 2,4,6-trisubstituted pyridines (**1–5**) were synthesized using a one-pot synthesis as shown in Equation 1. This simple synthetic route is advantageous in that it requires the use of fewer starting materials and less than half the reaction time of the more commonly used three-step method [8]. Asymmetrically substituted pyridines **6** and **7** were synthesized using a three-step reaction [8] as outlined in Scheme 1. In this scheme, a chalcone is synthesized as described in the literature [9–13] and reacted with an *N*-phenacylpyridinium salt to afford the asymmetrical product. Compound **1** has been previously described in the literature [14–16], but to the best of our knowledge, compounds **2–7** are novel.

Protonation studies. Protonation studies were carried out for all of the dyes using HCl and $HClO_4$ in acetonitrile (ACN). Absorption spectra from the studies using HCl have not been included in this section to avoid redundancy, as similar spectral behavior is observed in the presence of both acids. Two well-resolved equilibria are present in the protonation spectra, as indicated by two distinct sets of isosbestic points. These equilibria are generalized in Equation 2.

Because two distinct equilibria were present, the spectra were split into two groupings to simplify interpretation and avoid spectral crowding. The subsets of spectra belonging to group (I) correspond to the first protonation equilibrium (defined by pK_{a2}), and include spectra of the base form of the dye and of the dye in the presence of increasing concentrations of $HClO_4$, up to the maximum observed absorptivity for the red-shifted peak (typically 40–60 μM $HClO_4$), at which point the concentration of the singly protonated form is presumed to be at a maximum. The subsets of spectra belonging to group (II) correspond to the second protonation equilibrium (defined by pK_{a1}), and include spectra obtained by increasing the concentration of acid past that corresponding to the maximum observed absorptivity of the red-shifted peak. As similar protonation behavior occurs for all of the compounds, relevant peaks will be distinguished by the conventions α (for the peak around 280 nm), β (for the ICT peak around 340 nm), and χ (for the red-shifted protonation ICT peak around 440 nm).

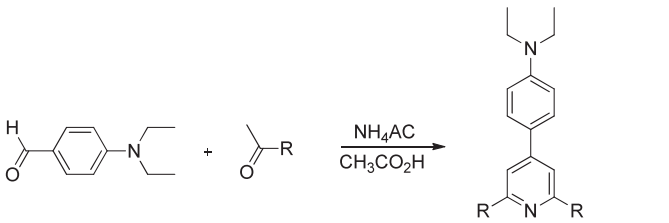

1: R = Phenyl
2: R = *p*-Tolyl
3: R = *p*-Chlorophenyl
4: R = β-Naphthyl
5: R = *tert*-Butyl

Equation 1. Synthetic route of symmetrical 2,4,6-trisubstituted pyridines.

Scheme 1. Synthetic route of asymmetrical 2,4,6-trisubstituted pyridines.

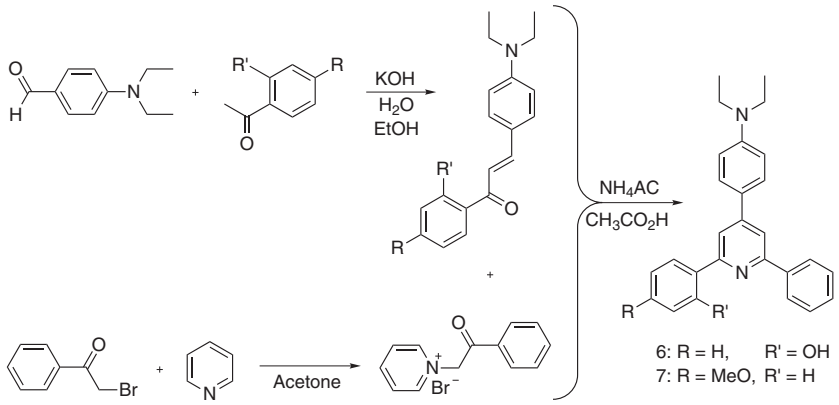

$$B \overset{pK_{a2}}{\leftrightarrow} HB^{+} \overset{pK_{a1}}{\leftrightarrow} H_2B^{2+}$$

Equation 2. General diprotic acid–base equilibrium.

Absorption spectra from the protonation study of compound **2** using $HClO_4$ are provided in Figure 1. The protonation behavior exhibited by this derivative is representative of the behavior exhibited by all of the aryl-substituted dyes except compound **6**, which will be discussed in the following paragraphs.

In the first equilibrium [group (I) spectra, characterized by pK_{a2}], upon adding increasing concentrations of acid, a decrease in the α band (around 290 nm for compound **2**) and a decrease and blue shift in the β band (initially present around 340 nm for compound **2**) is observed, whereas the red-shifted ICT χ band (around 440 nm for compound **2**) appears and increases to a maximum. This shift has been attributed to delocalization of the positive charge and increased conjugation within the π system of the molecule upon protonation [5], and the results in a visible color change from colorless to yellow. In group (II) spectra, the α band increases again; the β band undergoes a red-shift back to its original wavelength, and the χ band decreases in intensity (all the way to zero in the presence of high enough concentrations of acid). This behavior is associated with a disappearance of the yellow color.

Pyridine is known to display an absorption band at 270 nm because of the $\pi \rightarrow \pi^*$ excitation, and upon protonation, the intensity of absorption of this band increases without any appreciable spectral shift [17]. The λ_{MAX} of this absorption band coincides closely the α band of the compounds. Thus, it would seem that the increased absorptivity around 280 nm as acid concentrations are increased in the second equilibrium is also most likely attributable to pyridine protonation and the localization of charge associated with protonation of the second basic site. It was this observation that prompted the correlated NMR-absorption studies.

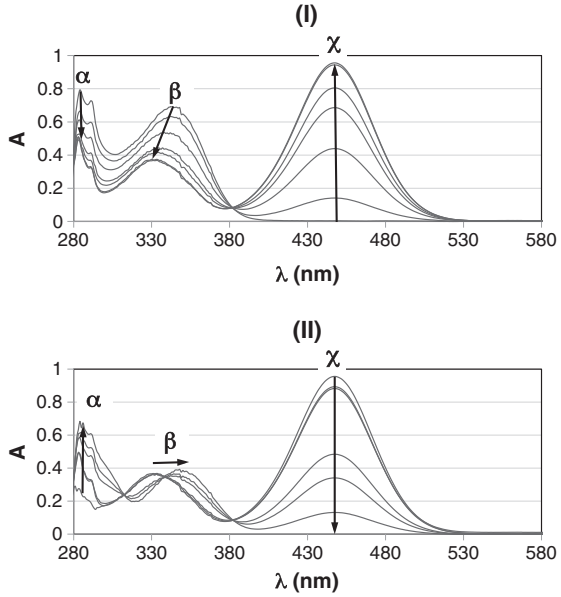

Figure 1. Protonation study of compound **2** using $HClO_4$, with labeled α, β, and χ bands. (I): 0–45 μM $HClO_4$, (II): 45–4000 μM $HClO_4$.

For alkyl substituted **5**, the spectral behavior was similar, but one important difference between its spectra and those of the aryl-substituted compounds was observed. Absorption spectra from the protonation study of dye **5** using $HClO_4$ are provided in Figure 2.

Similar spectral behavior was observed in the α and χ bands for both the aryl- and alkyl-substituted compounds. However, for the aryl-substituted compounds **1–4** and **7**, the β band is present throughout both protonation equilibria (spectral groupings (I) and (II)), whereas for alkyl substituted **5**, the β band decreases and disappears in the first equilibrium as the χ band increases and reaches its maximum. As acid concentrations are increased beyond the first equilibrium for derivative **5**, the χ band decreases to zero, and the intensity of the α band increases, but there is no reappearance of the β band. This behavior is

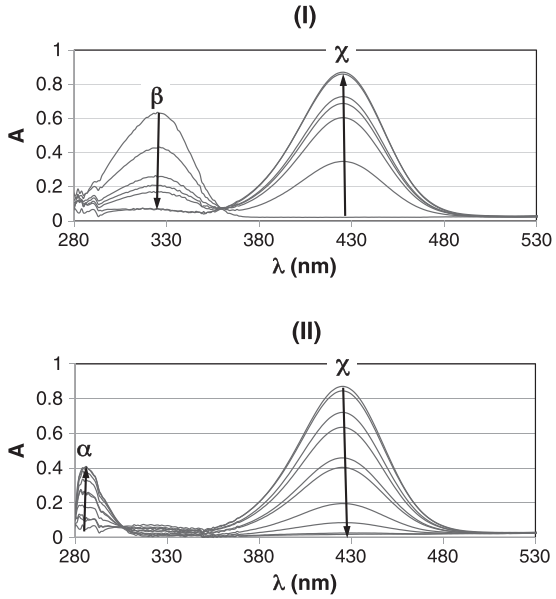

Figure 2. Protonation study of compound **5** using $HClO_4$, with labeled α, β, and χ bands. (I): 0–45 μM $HClO_4$, (II): 45–4000 μM $HClO_4$.

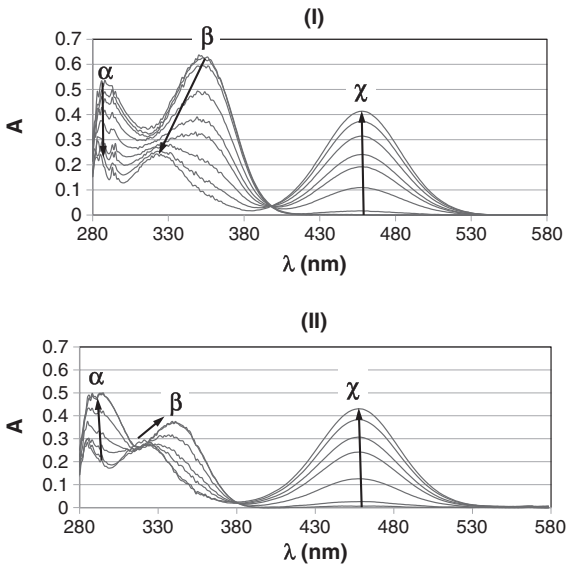

Figure 3. Protonation study of compound **3** using $HClO_4$, with labeled α, β, and χ bands. (I): 0–45 μM $HClO_4$, (II): 45–4000 μM $HClO_4$.

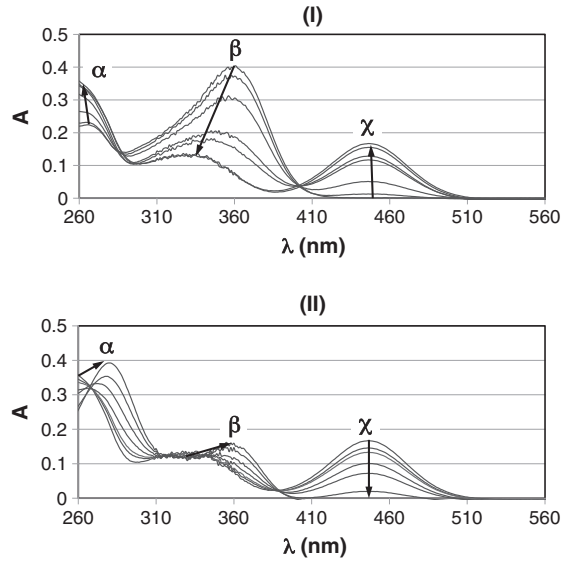

Figure 4. Protonation study of compound **6** using $HClO_4$, with labeled α, β, and χ bands. (I): 0–50 μM $HClO_4$, (II): 50–4000 μM $HClO_4$.

reversible upon addition of base and is therefore not due to dye oxidation or decomposition (as was initially thought when the spectra were first observed). The continuous presence of the β ICT band in all spectra for compounds with aryl substituents at the 2 and 6 positions (as contrasted with the disappearance of the β band in alkyl-substituted **5**) indicates that the 2 and 6 positions participate in the intramolecular charge transfer interaction in addition to the anilino substituent at the 4 position, acting as "secondary donors" of electron density to the pyridine nitrogen.

It is worth noting that most of the compounds display greater absorptivity in the bathochromic χ band relative to the base form β band when protonated with $HClO_4$; the only exceptions are compounds **3** and **6** (spectra provided in Figures 3 and 4, respectively). These two compounds are expected to be the least basic, poorest nucleophiles of the compounds studied, as derivative **3** possesses electron-withdrawing *para*-chlorophenyl substitution, and derivative **6** possesses an *ortho*-hydroxyphenyl moiety as its 2 position that is capable of intramolecular hydrogen bonding with the pyridine nitrogen and competing with external protons.

It is interesting to note that the spectra obtained from compound **6** (Figure 4) behaves somewhat differently than those obtained from all other aryl-substituted compounds. Specifically, in the other aryl-substituted compounds (**1–4** and **7**), the α band is present around 290 nm, decreases in group I spectra, and increases in group II spectra; whereas for compound **6**, the short wavelength absorption band (denoted a) is present at around 260 nm and increases in intensity in both group I and group II spectra (while exhibiting a red-shift in group II spectra). This difference in spectral behavior is potentially attributable to the intramolecular hydrogen bonding previously posited.

For protonation studies carried out using HCl, nearly identical spectral responses and patterns based on substitution were observed. The primary spectroscopic difference observed was that when HCl was used, the maximum absorptivity of the red-shifted χ band was substantially reduced for all compounds, as will be discussed further in the "solvent and acid effects" section.

Molar absorptivities of 2,4,6-trisubstituted pyridines. Average molar absorptivities of the ICT peaks corresponding to the singly protonated and nonprotonated

forms of the dyes are provided in Table 1, along with their standard deviations.

The standard deviations of the molar absorptivities indicated reasonably good reproducibility of the calculated values, with the highest %RSD corresponding to the base form of dye **3** (6.45%). Additionally, correlation coefficients indicated reasonably good linearity; the poorest R^2 value calculated was 0.998.

The base forms of these compounds had wavelengths of maximum absorption ranging from 287 to 352 nm, depending on substitution. Dyes with phenyl-based substitution at the 2 and 6 positions had a comparatively narrow range of λ_{MAX} between 343 and 359, despite variation of the phenyl substitution. Dye **5**, which possesses *tert*-butyl substituents in place of the aryl groups possessed by all the other dyes studied, exhibits a shorter λ_{MAX} (326 nm). This is to be expected given that alkyl substituents at the 2 and 6 positions of the pyridine ring cannot contribute to the energy-lowering conjugation that aryl substituents participate in.

]The spectral behavior discussed with respect to protonation studies can also be observed in this data. The red-shifted protonation peak absorptivity shows a strong dependence on the substitution of the compounds, but the basic ICT peak does not demonstrate any clear pattern of dependence on substitution. In general, compounds with electron-donating substituents (e.g. **2**, **5**, and **7**) possess much higher protonation peak absorptivities, whereas compounds with electron-withdrawing or hydrogen-bonding substituents (e.g. **3** and **6**) possess substantially lower absorptivities. Notably, this increase in absorptivity for compounds with electron-donating substitution is observed both for compounds with substituents that donate electrons either by inductive effects (**5**) or by resonance effects (**7**).

Solvent and acid effects. Another interesting observation from these studies was that both the protonating acid and the solvent choice strongly affects the absorptivity of the bathochromic peak correlated to the singly protonated form of the dye, but not that of the base form. A summary of the average molar absorptivities of the ICT peaks corresponding to the nonprotonated basic forms of compounds **1–3** in different solvent systems relevant to this study is provided in Table 2, along with standard deviations.

It is interesting to note that the base form peaks for the compounds did not show any pronounced dependence of absorptivity on solvent. There was a very slight solvatochromic shift in wavelength observed for all of these dyes, with ACN solutions resulting in the shortest wavelengths, ethanol–water mixtures intermediate, and DMSO solutions resulting in the longest wavelengths of maximum absorption.

A summary of the average molar absorptivities of the red-shifted ICT peaks corresponding to the singly protonated forms of compounds **1–3** in different solvent systems relevant to this study is provided in Table 3, along with standard deviations. Note that $HClO_4$ was not used with DMSO as a solvent because of the potential for explosive oxidation reactions [18]. Note also that the 50% EtOH/H_2O (*v*/*v*) solvent system with $I = 0.1M$ and $HClO_4$ as a protonating acid was chosen to replicate the conditions used in the spectroscopic pK_a determination.

As previously mentioned, when $HClO_4$ is used as the protonating acid, there is an increase in the observed absorptivity of the red-shifted peak corresponding to the

Table 2

Average molar absorptivities of nonprotonated compounds **1–3** in acetonitrile (ACN), DMSO, and 50% EtOH/H_2O (*v*/*v*).

Compound	Solvent	λ_{MAX} (nm)	$\varepsilon(\lambda_{MAX})$ (M^{-1} cm^{-1})
1	ACN	347	$(2.48 \pm 0.015) \times 10^4$
	DMSO	354	$(3.24 \pm 0.020) \times 10^4$
	50% EtOH/H_2O[a]	350	$(2.84 \pm 0.011) \times 10^4$
2	ACN	344	$(3.48 \pm 0.091) \times 10^4$
	DMSO	349	$(2.90 \pm 0.099) \times 10^4$
	50% EtOH/H_2O[a]	347	$(2.82 \pm 0.095) \times 10^4$
3	ACN	352	$(2.7 \pm 0.18) \times 10^4$
	DMSO	362	$(2.52 \pm 0.039) \times 10^4$
	50% EtOH/H_2O[a]	358	$(2.6 \pm 0.20) \times 10^4$

[a] $I = 0.1M$

Table 1

Wavelengths of maximum absorption (λ_{MAX}) and molar absorptivities (ε) of protonated and nonprotonated 2,4,6-trisubstituted pyridines. Molar absorptivities of protonated form given for bathochromic peak in [HCl] associated with maximum extent of bathochromic absorptivity observed.

Compound	Substituent (position)		Base form (B) in ACN		Singly protonated form (HB^+) in HCl/ACN (<0.1% H_2O)	
	2	6	λ_{MAX} (nm)	$\varepsilon(\lambda_{MAX})$ (M^{-1} cm^{-1})	λ_{MAX} (nm)	$\varepsilon(\lambda_{MAX})$ (M^{-1} cm^{-1})
1	Ph	Ph	347	$(2.48 \pm 0.015) \times 10^4$	450	$(2.2 \pm 0.13) \times 10^4$
2	*p*-Tolyl	*p*-Tolyl	344	$(3.48 \pm 0.091) \times 10^4$	448	$(4.06 \pm 0.018) \times 10^4$
3	*p*-ClPh	*p*-ClPh	352	$(2.7 \pm 0.18) \times 10^4$	456	$(8.7 \pm 0.41) \times 10^3$
4	β-Np	β-Np	349	$(3.54 \pm 0.019) \times 10^4$	456	$(2.56 \pm 0.010) \times 10^4$
5	*tert*-Butyl	*tert*-Butyl	326	$(3.0 \pm 0.20) \times 10^4$	425	$(4.12 \pm 0.050) \times 10^4$
6	*o*-OHPh	Ph	359	$(3.39 \pm 0.026) \times 10^4$	447	$(5.8 \pm 0.15) \times 10^3$
7	Ph	*p*-MeOPh	343	$(3.58 \pm 0.070) \times 10^4$	448	$(3.77 \pm 0.076) \times 10^4$

Ph, phenyl; β-Np, β-naphthalene; *o*-OHPh, *o*-hydroxyphenyl; *p*-MeOPh, *p*-methoxyphenyl; *p*-ClPh, *p*-chlorophenyl; ACN, acetonitrile.

Table 3

Average molar absorptivities of singly protonated compounds **1–3** in acetonitrile (ACN), DMSO, and 50% EtOH/H_2O (*v*/*v*), $I = 0.1M$.

Compound	Solvent	Acid	[Acid] (μM)	λ_{MAX} (nm)	$\varepsilon(\lambda_{MAX})$ (M^{-1} cm^{-1})
1	ACN	$HClO_4$	4.00E + 01	449	$(2.99 \pm 0.066) \times 10^4$
	ACN	HCl	4.10E + 01	450	$(2.2 \pm 0.13) \times 10^4$
	DMSO	HCl	1.00E + 04	447	$(7.56 \pm 0.097) \times 10^3$
	50% EtOH/H_2O[a]	$HClO_4$	1.20E + 03	453	$(6.7 \pm 0.34) \times 10^3$
2	ACN	$HClO_4$	4.60E + 01	447	$(4.8 \pm 0.12) \times 10^4$
	ACN	HCl	4.10E + 01	448	$(4.06 \pm 0.018) \times 10^4$
	DMSO	HCl	1.00E + 04	446	$(1.23 \pm 0.010) \times 10^4$
	50% EtOH/H_2O[a]	$HClO_4$	8.51E + 02	451	$(1.25 \pm 0.010) \times 10^4$
3	ACN	$HClO_4$	5.00E + 01	456	$(1.90 \pm 0.064) \times 10^4$
	ACN	HCl	5.13E + 01	456	$(8.7 \pm 0.41) \times 10^3$
	DMSO	HCl	1.00E + 04	452	$(1.33 \pm 0.010) \times 10^3$
	50% EtOH/H_2O[a]	$HClO_4$	2.57E + 03	456	$(9.9 \pm 0.38) \times 10^2$

[a] $I = 0.1M$

singly protonated form for all compounds relative to those absorptivities measured using HCl as the protonating acid. This behavior is apparent in the data provided in Table 3 for HCl and $HClO_4$ in ACN. The reason for this difference in absorptivity is presumably increased association between the conjugate anion of the acid and the protonated compounds in the case of weaker acids [5]. Hydrochloric acid behaves as a weak acid in ACN (pK_a 8.9) [19] and is not fully dissociated, whereas perchloric acid behaves as a strong acid and is known to be fully dissociated in ACN [20]. It follows that the conjugate perchlorate anion would be less associated with the protonated compounds than the chloride anion; therefore as chloride is more likely to associate and assist in charge stabilization, the extent of charge transfer within the protonated compounds would be reduced [5].

The data provided in Table 3 also indicates that solvent choices also substantially affected the absorptivities of the red-shifted ICT peak correlated to the singly protonated form of the dye. When the data for HCl in ACN is compared with that obtained using HCl in DMSO, there is a substantial decrease in the observed absorptivity for compounds **1** (66%), **2** (70%), and **3** (85%). Similarly, when the data for $HClO_4$ in ACN is compared with that obtained using $HClO_4$ in 50% EtOH-H_2O, there is a substantial decrease in the observed absorptivity for compounds **1** (78%), **2** (74%), and **3** (95%). It can be generalized that the absorptivity seems to decrease with increasing dielectric constant of the solvent or solvent mixture. It should be noted that no substantial shift in wavelength is observed in the protonation spectra upon changing solvents; however, the hypochromic effect observed in more polar solvents does indicate solvatochromic properties, as would be expected given the dipolar nature of the protonated state [6]. The hypochromic effect observed may be due to increased dipole-dipole interactions between the charged protonated form of the compounds and the polar solvent molecules. These observations indicate that solvents must be chosen carefully when metal-binding or protonation studies are carried out.

Spectroscopic pK_a determination. The spectral results of the pK_a studies of compound **2** in 50% EtOH/H_2O are provided in Figure 5. For ease of interpretation and to avoid crowded spectra, the spectra have again been grouped into two plots, the first plot (I) depicting spectra corresponding to the first protonation equilibrium (pK_{a2}), and the second plot (II) depicting spectra corresponding to the second protonation equilibrium (pK_{a1}). In both spectra, arrows indicate the spectral changes associated with decreasing pH.

Both equilibria in both sets of spectra show clear isosbestic behavior, reinforcing the assumption that the pK_a values are at least two units apart and validating the approach to calculating pK_a used in this section. Furthermore, the absorption of the red-shifted peak at 449 nm goes from zero

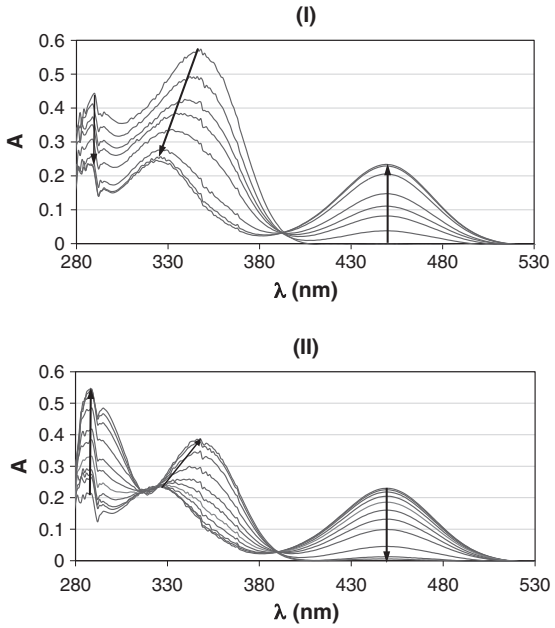

Figure 5. Absorption spectra from pK_a determination of compound **2** in 50% EtOH/H_2O (25°C, $I = 0.100M$ except for pH < 1.00). (I) pH 6.18–3.20, (II) pH 3.20–0.92.

to a maximum in the first equilibrium and decreases back to zero in the second equilibrium, further validating the approach for calculating pK_a. The absorption at 449 nm was plotted as a function of pH; this plot is provided in Figure 6.

Provided in Table 4 are the experimentally determined p_sK_a values for the compounds in 50% EtOH/H_2O. The data in Table 4 indicates that when electron-donating substituents (such as *p*-tolyl) are interchanged for electron-withdrawing substituents (such as *p*-chlorophenyl) at the 2 and 6 positions of pyridine, neither the p_sK_{a1} nor the p_sK_{a2} are decreased substantially (the decrease for both in this case is approximately 0.4–0.5 units). Interestingly, the p_sK_{a1} of "intermediate" phenyl-substituted **1** was actually observed to be below that of the more electron-withdrawing chlorophenyl-substituted **3**, whereas the p_sK_{a2} is closer to that of electron-donating tolyl-substituted **2**. This modulation of pK_a by changing substitution more or less follows the expected pattern (as electron-withdrawing substituents are expected to make the dye less basic), but the observed change in pK_a is not as large as was expected, especially given the large differences in absorptivity of the protonation peak between those compounds with electron-donating substitution and those with electron-withdrawing substitution. One potential explanation for this relatively minor change in pK_a is stabilization by the electron-donating diethylamino aryl group at the 4-position of the pyridine ring.

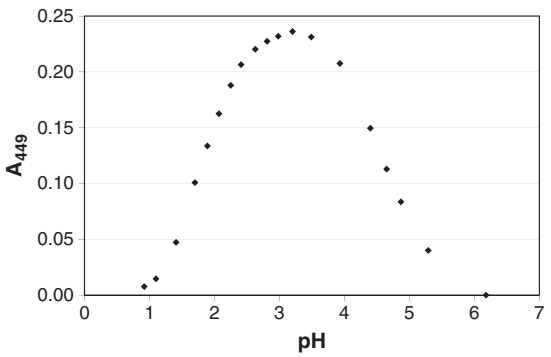

Figure 6. Absorption of compound **2** at 449 nm as a function of pH from pK_a determination in 50% EtOH/H_2O (25°C, $I = 0.100M$ except for pH < 1.00).

Table 4

Calculated p_sK_a values in 50% EtOH/H_2O, $I = 0.1M$.

Compound	Substituents (2 and 6)	p_sK_{a1}	p_sK_{a2}
1	Phenyl	1.31 ± 0.081	4.5 ± 0.12
2	*p*-Tolyl	1.84 ± 0.031	4.63 ± 0.010
3	*p*-Chlorophenyl	1.34 ± 0.099	4.2 ± 0.12

Correlated NMR-absorption studies. Provided in Figure 7 is the structure of compound **1** with diagnostic proton positions "a, b, c" (proximal and/or conjugated to either of the basic nitrogen atoms) labeled. Provided in Table 5 are the results of the correlated NMR-absorption study at 25°C, including the absorption at 450 nm (red-shifted ICT peak corresponding to the singly protonated form), chemical shifts of diagnostic positions in the molecule, changes in chemical shift of diagnostic positions in the molecule relative to the nonprotonated form of **1**, concentrations of acid in each sample, and calculated pH (p_cH). The p_cH value was calculated assuming the activity of the hydrogen ion is unity ($p_cH = -\log[H^+] = -\log[HClO_4]$). It should be noted that equating $[H^+]$ with $[HClO_4]$ is valid given that perchloric acid is known to be fully dissociated in ACN [14]. In Table 5, the first three samples correspond to the first equilibrium, and the last two correspond to the second; the fourth sample corresponds to the maximum concentration of the singly protonated species. Provided in Figure 8 is a graphic representation of the data provided in Table 5, wherein change in chemical shift for diagnostic positions a, b, and c is plotted as a function of p_cH. In this representation, the line at p_cH 3.26 represents the division between the first and second protonation equilibria. Note that NMR studies carried out at higher (37°C) and lower (0°C) temperatures resulted in the same outcome.

It is readily apparent from Table 5 and Figure 8 that the majority of the change in chemical shift for the protons in proximity with and conjugated directly to the pyridine nitrogen (positions b and c) occurs within the first equilibrium, whereas the chemical shift for position a (inductively coupled and α to the aniline nitrogen) does not change substantially until the second equilibrium. This provides strong evidence supporting protonation of the pyridine ring in the first equilibrium (pK_{a2}) and protonation of the aniline nitrogen in the second equilibrium (pK_{a1}).

The finding that the pyridine nitrogen is protonated prior to the aniline nitrogen supports the discussion of the spectroscopic behavior provided in the "protonation studies" section. If pyridine is protonated first, the positive charge is delocalized throughout the conjugated chromophore, as illustrated in Figure 9. Delocalization of a positive charge

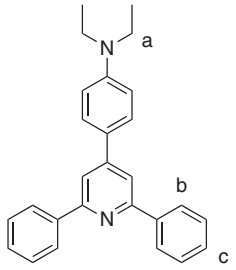

Figure 7. Structure of **1** with diagnostic positions a, b, and c labeled.

Table 5

Chemical shifts (δ) and changes in chemical shift relative to nonprotonated form of **1** (Δδ) for diagnostic positions a, b, and c (Figure 7), absorption at 450 nm (A_{450}), concentration of $HClO_4$ in samples and calculated pH (p_cH) from correlated NMR-absorption study at 25°C.

$[H^+]$ (mM)	p_cH	A_{450}	Diagnostic chemical shifts (δ) and change in chemical shift (Δδ)					
			δ a (ppm)	δΔ a (ppm)	δ b (ppm)	δΔ b (ppm)	δ c (ppm)	δΔ c (ppm)
0.000	N/A	0	3.4566	0.0000	8.2640	0.0000	7.4775	0.0000
0.100	4.00	0.585	3.4691	0.0125	8.2173	0.0468	7.5255	0.0480
0.300	3.52	2.136	3.4842	0.0276	8.0988	0.1652	7.5953	0.1178
0.550	3.26	3.254	3.4873	0.0307	8.0233	0.2407	7.6720	0.1945
1.000	3.00	0.685	3.6391	0.1825	8.0163	0.2478	7.7017	0.2242
5.000	2.30	0	3.7115	0.2549	8.0159	0.2481	7.7231	0.2456

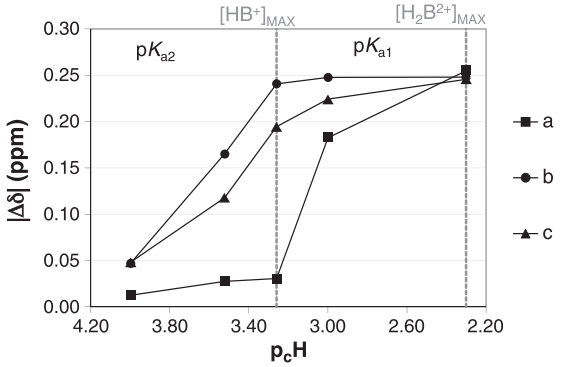

Figure 8. Absolute value of change in chemical shift for diagnostic positions a, b, and c (Figure 7) as a function of p_cH with included division between first and second equilibrium (dashed line labeled $[HB^+]_{MAX}$)and marker indicating p_cH at which all of **1** is in the doubly protonated form (dashed line labeled $[H_2B^{2+}]_{MAX}$).

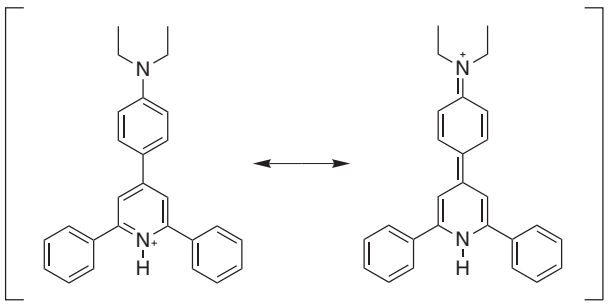

Figure 9. Representative resonance structures illustrating charge delocalization resulting from pyridine protonation.

across a conjugated system is known to result in a red-shifted absorption peak and higher absorptivity relative to that of an uncharged system with the same extent of conjugation, as is exemplified by other common classes of dyes such as the cyanines [21]; this would readily explain the observed bathochromic shift and increased absorptivity in spectra associated with the first protonation equilibrium. Moreover, this delocalization of charge is impossible if the aniline nitrogen is protonated first. In the second equilibrium, both nitrogen atoms become protonated, and resonance delocalization is no longer possible. The disappearance of the red-shifted peak and the increase in blue-shifted peak absorptivity in spectra corresponding to the second equilibrium is likely explained by this "relocalization" of charges when both nitrogen atoms are positively charged.

CONCLUSIONS

All compounds presented in this study were synthesized, purified, and isolated in a good yield, then characterized by ^{1}H-NMR and ^{13}C-NMR. Protonation studies indicate that each of these compounds displays a bathochromic shift of approximately 100 nm upon addition of acid, with a marked corresponding color change (λ_{MAX} = 425–456 nm, Table 1). Preliminary studies on the effect of varying the substituent at the 4 position indicate that the amino nitrogen of the diethylaminoaryl substituent is responsible for the magnitude of this red shift (relative to alkyl- and alkoxy-substituted compounds, data not shown). Upon further addition of acid to these compounds, there is a reversal of the color change and a corresponding hypsochromic shift, with the new peak demonstrating a λ_{MAX} around 270–280 nm. The presence of clear isosbestic points suggests that these two protonation equilibria are distinct and well-resolved (i.e. pK_{a1} and pK_{a2} are separated by at least two pH units); results of pK_a studies confirm this finding. Correlated NMR-absorption studies support the presumption that the pyridine nitrogen is in fact the site of the first protonation (pK_{a2}). Accordingly, the bathochromic shift is likely attributable to resonance delocalization of the positive charge throughout the chromophore.

Substitution with electron-donating groups was correlated to an increase in the absorptivity of the red-shifted protonation peak, which may be explained in terms of charge transfer behavior; as the electron-donating nature of the substituents increases, more extensive delocalization of the positive charge throughout the structure is possible, resulting in a greater absorptivity. Surprisingly, despite the large differences in protonation peak absorptivity observed upon varying substitution, the observed pK_a values are not strongly modulated by interchanging

electron-withdrawing substituents for electron-donating substituents at the 2 and 6 positions of the pyridine ring.

The solvent and the protonating acid also both have a strong influence on the absorptivity of the bathochromic protonation peak. Absorptivities of the protonation peak in ACN were substantially higher than those found in either DMSO or 50% EtOH/H_2O when the same protonating acid was used. Additionally, it was found that in ACN, $HClO_4$ resulted in greater bathochromic peak absorptivity than HCl, presumably because of increased association of the conjugate anion of weaker acids with the protonated compounds.

In this study, structural features of 2,4,6-trisubstituted pyridines that affect the amplitude of spectroscopic response to cations for applications as pH indicators and ion probes have been determined and rationalized on the basis of known spectroscopic phenomena. These findings should assist in the future design of donor–acceptor pyridine ion probes with optimal spectroscopic and color indicating responses for applications as color indicators of ions.

EXPERIMENTAL

Instrumentation. Absorption spectra were measured using either a Perkin-Elmer Lambda 20 UV–vis-NIR Spectrophotometer (Perkin-Elmer Incorporated, Waltham, MA) or a Cary 3G UV–vis Spectrophotometer (Agilent Technologies Incorporated, Santa Clara, CA). Disposable Fisherbrand polystyrene cuvettes with pathlengths of 1.00 cm were obtained from Fisher Scientific (Fairlawn, NJ), and quartz cuvettes of 1.000 cm pathlength were obtained from Starna Cells, Inc. (Atascadero, CA). A quartz cuvette of 0.200 cm pathlength (and a spacer to adjust the effective sample compartment size) was obtained from NSG Precision Cells (Farmingdale, NY) for the correlated absorption-NMR studies. A ROSS pH electrode (operational pH range: 0–14; Orion Research, Inc., Beverly, MA) was used for pH measurements and calibrated using a three-point calibration method with pH 4.00, pH 7.00, and pH 10.00 reference standard buffer solutions (EMD Millipore, Billerica, MA). All calculations were carried out using Microsoft Excel (Microsoft Corporation, Redmond, WA). RT (25°C) and higher temperature (37°C) NMR studies were carried out on a 400 MHz Bruker Avance NMR spectrometer (Bruker BioSpin Corporation, Billerica, MA). The lower temperature (0°C) NMR study was carried out on a 600 MHz Bruker Avance NMR spectrometer. NMR spectra were processed using Topspin Software (Bruker BioSpin Corporation, Billerica, MA). Standard 5 mm NMR tubes were obtained from Wilmad-LabGlass (Vineland, NJ).

Chemicals and reagents. Perchloric acid ($HClO_4$; 69.5%, Lot No. 02829ER) was obtained from Aldrich Chemical Co. (Milwaukee, WI). Hydrochloric acid (HCl; 12.309*M*) and DMSO (≥99.8%, UV grade) were obtained from Sigma-Aldrich (St. Louis, MO). Sodium chloride (NaCl; 99 + %) and ACN (99.9% and 0.03% H_2O) were obtained from Thermo Fisher Scientific (Waltham, MA). ACN was stored over freshly dried 4 Å molecular sieves. Type 1 ultrapure water (18.2*M*Ω cm) was obtained from a Barnstead Nanopure Water System (Thermo Fisher Scientific). Koptec ethanol (EtOH; 200 proof; 99.5% min) was obtained from VWR (Radnor, PA). Deuterated DMSO (DMSO-d_6; 99.9% D +0.05% V/V TMS) and deuterated ACN (CD_3CN; 99.8% D) were obtained from Cambridge Isotope Laboratories (Andover, MA) and stored under dry N_2 (Airgas, Inc., Radnor, PA). All of the 2,4,6-trisubstituted pyridines were synthesized in our lab. Purities were verified by ^{1}H-NMR, ^{13}C-NMR, and mp ranges. ^{1}H-NMR spectra have been provided in the Supporting Information, Figures S.1–S.7, and ^{13}C-NMR spectra provided in the Supporting Information, Figures S.8–S.14.

General procedure for preparation of symmetrical 2,4,6-trisubstituted pyridines. Symmetrically substituted 2,4,6-trisubstituted pyridines (**1–5**) were synthesized using a one-pot synthesis as shown in Equation 1. In this one-pot synthesis, 1 equiv of 4-diethylaminobenzaldehyde (40 mmol), 2 equiv of variously substituted methyl ketones (80 mmol), and 2 equiv of ammonium acetate (80 mmol) were mixed together in a 250-mL round-bottomed flask, followed by addition of a catalytic amount of acetic acid. The reaction mixture was heated for 24 h at 100°C to obtain the 2,4,6-trisubstituted pyridine product. TLC was performed to monitor the extent of reaction, and upon completion, 200 mL of a saturated solution of sodium carbonate was added to quench the reaction. The reaction mixture was extracted with dichloromethane to isolate the product, and the organic layer was washed three times with water. After the washing steps, the organic layer was dried over anhydrous magnesium sulfate, which was removed by filtration. The filtrate was concentrated under vacuum and further purified by column chromatography on silica gel using dichloromethane/hexanes as eluent. Yield: 58–76%.

General synthesis of unsymmetrical 2,4,6-trisubstituted pyridines. Asymmetrically substituted pyridines **6** and **7** were synthesized using a three-step synthesis. In the first step, a chalcone was synthesized by reacting a substituted acetophenone (80 mmol) with 4-diethylaminobenzaldehyde (80 mmol) in a 250-mL round-bottomed flask containing 40 mL ethanol. The reaction was heated for 10 min, and then 40 mL of a 55% potassium hydroxide solution was added slowly with stirring. The reaction mixture was left for an additional 24 h with continuous stirring. TLC was performed to monitor the extent of reaction, and upon completion, the reaction mixture was extracted with dichloromethane to isolate the product. The organic layer was washed three times with water, and then dried over anhydrous magnesium sulfate, which was removed by filtration. The filtrate was then concentrated under vacuum to isolate the desired chalcones. Yield: 76–83%.

In the second step, an *N*-phenacylpyridinium salt was synthesized by combining 2-bromoacetophenone (80 mmol) and anhydrous pyridine (160 mmol) in 200 mL acetone in an Erlenmeyer flask and stirring continuously for 48 h at RT, until a chunky, milky precipitate formed. The resulting product was diluted with diethyl ether (200 mL) and then filtered. The filtrand was washed with diethyl ether and dried under vacuum to furnish the desired product as a colorless solid. Yield: 91%.

In the third step, unsymmetrical 2,4,6-trisubstituted pyridine derivatives were synthesized by combining the chalcone from step 1 (40 mmol) and the *N*-phenacylpyridinium salt from step 2 (40 mmol) in a 500-mL round-bottomed flask in the presence of glacial acetic acid (120 mL) and ammonium acetate (NH_4Ac, 60 g). The reaction was stirred under reflux for 24 h. TLC was performed to monitor the extent of reaction, and upon completion, the reaction mixture was poured into 400 mL of water and made basic with sodium hydroxide. The reaction mixture was extracted with dichloromethane to isolate the product, and the organic layer was washed three times with water. After the washing steps, the organic layer was dried over anhydrous magnesium sulfate, which

was removed by filtration. The filtrate was concentrated under vacuum to give a brown oil residue and further purified by column chromatography on silica gel using dichloromethane/hexanes as eluent. Yield: 52–57%.

Thin layer chromatography. Normal phase TLC was carried out periodically to determine the extent of reaction and the purity of the compounds. The ideal mobile phase for both TLC and column chromatography was determined by starting with a 50:50 mixture of hexane and dichloromethane, then adjusting the polarity as needed to achieve the desired separation of compounds.

Column chromatography. Normal phase column chromatography using a mixture of dichloromethane and hexanes was carried out to purify pyridine derivatives (**1–7**). The column was packed as a slurry using hexanes, and this solvent was eluted prior to loading the crude product. The crude products were dissolved in dichloromethane and loaded on the column, and a mobile phase half the polarity of the TLC mobile phase was run through the column; as elution slowed, the mobile phase polarity was increased to that of the mobile phase used for TLC to obtain optimal separation within the column.

4-(2,6-Diphenylpyridin-4-yl)-N,N-diethylaniline (1). Yellow-orange solid, mp 96–97°C, yield: 8.8 g (58%); TLC (70:30 CH_2Cl_2/Hexanes) $R_f = 0.43$; ^{1}H-NMR (400 MHz, DMSO-d_6) δ (ppm): 1.15 (t, $J = 7.0$ Hz, 6H), 3.43 (q, $J = 7.0$ Hz, 4H), 6.80 (d, $J = 8.6$ Hz, 2H), 7.47 (t, $J = 7.1$ Hz, 2H), 7.55 (t, $J = 7.5$ Hz, 4H), 7.90 (d, $J = 8.6$ Hz, 2H), 8.09 (s, 2H), 8.30 (d, $J = 7.5$ Hz, 4H); ^{13}C-NMR (100 MHz, DMSO-d_6) δ (ppm): 11.9, 43.2, 111.0, 114.3, 122.7, 126.3, 127.7, 128.2, 128.5, 138.6, 147.8, 148.9, 155.7.

4-[2,6-Bis(4-methylphenyl)pyridin-4-yl]-N,N-diethylaniline (2). Light yellow powdery crystals, mp 133–134°C, yield: 10.6 g (65%); TLC (70:30 CH_2Cl_2/Hexanes) $R_f = 0.43$; ^{1}H-NMR (400 MHz, DMSO-d_6) δ (ppm): 1.14 (t, $J = 7.0$ Hz, 6H), 2.39 (s, 6H), 3.42 (q, $J = 7.0$ Hz, 4H), 6.79 (d, $J = 9.0$ Hz, 2H), 7.34 (d, $J = 8.1$ Hz, 4H), 7.87 (d, $J = 9.0$ Hz, 2H), 8.02 (s, 2H), 8.19 (d, $J = 8.1$ Hz, 4H); ^{13}C-NMR (100 MHz, DMSO-d_6) δ (ppm): 12.5, 20.9, 43.7, 111.5, 114.2, 123.4, 126.7, 128.2, 129.3, 136.5, 138.5, 148.2, 149.3, 156.1.

4-[2,6-Bis(4-chlorophenyl)pyridin-4-yl]-N,N-diethylaniline (3). Light yellow powdery crystals, mp 174–176°C, yield: 12.5 g (70%); TLC (70:30 CH_2Cl_2/Hexanes) $R_f = 0.73$; ^{1}H-NMR (400 MHz, DMSO-d_6) δ (ppm): 1.14 (t, $J = 7.0$ Hz, 6H), 3.43 (q, $J = 7.0$ Hz, 4H), 6.79 (d, $J = 9.0$ Hz, 2H), 7.60 (d, $J = 7.7$ Hz, 4H), 7.92 (d, $J = 9.0$ Hz, 2H), 8.14 (s, 2H), 8.35 (d, $J = 6.8$ Hz, 4H); ^{13}C-NMR (100 MHz, DMSO-d_6) δ (ppm): 12.5, 43.7, 111.4, 115.0, 122.9, 128.3, 128.6, 133.9, 137.8, 148.4, 149.7, 155.0.

4-[2,6-Bis(2-naphthyl)pyridin-4-yl]-N,N-diethylaniline (4). Finely divided orange crystals, mp 196–198°C, yield: 14.6 g (76%); TLC (70:30 CH_2Cl_2/Hexanes) $R_f = 0.60$; ^{1}H-NMR (400 MHz, DMSO-d_6) δ (ppm): 1.17 (t, $J = 7.0$ Hz, 6H), 3.46 (q, $J = 7.0$ Hz, 4H), 6.85 (d, $J = 9.0$ Hz, 2H), 7.57–7.62 (m, 4H), 7.99–8.02 (m, 4H), 8.10–8.16 (m, 4H), 8.32 (s, 2H), 8.57 (dd, $J = 8.6$, 1.7 Hz, 2H), 8.93 (s, 2H); ^{13}C-NMR (100 MHz, DMSO-d_6) δ (ppm): 12.5, 43.77, 111.5, 115.3, 123.2, 124.8, 126.1, 126.4, 126.7, 127.6,128.2, 128.3, 128.7, 133.2, 133.3, 136.6, 148.4, 149.5, 156.2.

4-[2,6-Bis(tert-butyl)-4-pyridinyl]-N,N-diethylaniline (5). White powdery crystals, mp 95–97°C, yield: 9.7 g (72%); TLC (70:30 CH_2Cl_2/Hexanes) $R_f = 0.10$; ^{1}H-NMR (400 MHz, DMSO-d_6) δ (ppm): 1.12 (t, $J = 6.7$ Hz, 6H), 1.35 (s, 18H), 3.38 (q, $J = 6.7$ Hz, 4H), 6.75 (d, $J = 8.5$ Hz, 2H), 7.31 (s, 2H), 7.58 (d, $J = 8.5$ Hz, 2H); ^{13}C-NMR (100 MHz, DMSO-d_6) δ (ppm): 12.4, 30.1, 37.3, 43.7, 111.6, 112.0, 124.7, 127.8, 147.8, 148.0, 167.1.

4-[2-(2-Hydroxyphenyl)-6-phenylpyridin-4-yl]-N,N-diethylaniline (6). Yellow solid, mp 140–142°C, yield: 9.0 g (57%); TLC (70:30 CH_2Cl_2/Hexanes) $R_f = 0.40$; ^{1}H-NMR (400 MHz, DMSO-d_6) δ (ppm): 1.15 (t, $J = 7.0$ Hz, 6H), 3.44 (q, $J = 7.0$ Hz, 4H), 6.81 (d, $J = 8.9$ Hz, 2H), 6.94–6.98 (m, 2H), 7.34 (t, $J = 7.8$ Hz, 1H), 7.54 (t, $J = 7.2$ Hz, 1H), 7.60 (t, $J = 7.6$ Hz, 2H), 7.96 (d, $J = 8.9$ Hz, 2H), 8.08 (d, $J = 7.6$ Hz, 2H), 8.10 (s, 1H), 8.28 (d, $J = 7.2$ Hz, 1H), 8.32 (s, 1H); ^{13}C-NMR (100 MHz, DMSO-d_6) δ (ppm): 12.5, 43.7, 111.4, 113.8, 115.2, 117.8, 118.8, 119.1, 122.5, 126.7, 127.5, 128.6, 129.2, 129.6, 131.3, 137.9, 148.6, 150.5, 154.1, 157.2, 159.4.

4-[2-(4-Methoxyphenyl)-6-phenylpyridin-4-yl]-N,N-diethylaniline (7). White powdery crystals, mp 92–94°C, yield: 8.5 g (52%); TLC (70:30 CH_2Cl_2/Hexanes) $R_f = 0.17$; ^{1}H-NMR (400 MHz, DMSO-d_6) δ (ppm): 1.14 (t, $J = 7.0$ Hz, 6H), 3.42 (q, $J = 7.0$ Hz, 4H), 6.79 (d, $J = 9.0$ Hz, 2H), 7.09 (d, $J = 8.9$ Hz, 2H), 7.47 (t, $J = 7.3$ Hz, 1H), 7.54 (t, $J = 7.7$ Hz, 2H), 7.88 (d, $J = 8.9$ Hz, 2H), 8.02 (s, 2H), 8.25–8.30 (m, 4H); ^{13}C-NMR (100 MHz, DMSO-d_6) δ (ppm): 12.0, 43.2, 54.7, 111.0, 113.5, 113.6, 122.9, 126.3, 127.7, 128.1, 128.4, 131.1, 138.8, 147.7, 148.8, 155.4, 155.5, 159.6

Protonation studies and method of determining molar absorptivities. For the protonation studies, working solutions of all dyes were prepared containing 20 μM dye and varied concentrations of acid (typically 20–200 μM) with negligible (<0.1%) added water, and the absorption spectra were measured. In ACN, studies were carried out using both $HClO_4$ and HCl for all of the dyes. For derivatives **1–3**, additional protonation studies were carried out using HCl in DMSO and $HClO_4$ in 50% EtOH/H_2O (*v*/*v*).

The absorption spectra of working solutions of varying dye concentrations were measured, and the absorption at a particular wavelength of maximum absorption (λ_{MAX}) was determined. The absorption of each sample at λ_{MAX} was plotted as a function of concentration; the linear regression equation was computed, and the molar absorptivity (ε) was taken as the slope, as per Beer's law. Absorptivities were determined in duplicate and averages, and percent relative standard deviations were calculated. Molar absorptivities for the basic forms of all of the dyes were determined in ACN. Absorptivities for the singly protonated forms of all compounds were determined by adding a constant amount of HCl in ACN to the solutions and taking the absorption at the bathochromic peak λ_{MAX} corresponding to the singly protonated form of the compound. Preliminary protonation studies using HCl were used to determine the concentration of HCl resulting in the greatest observed bathochromic peak absorptivity; this concentration of HCl was held constant, whereas the dye concentration was decreased to determine the protonated form molar absorptivity. Final working solutions contained <0.1% additional added H_2O from the HCl. For clarity, representative spectra and plots of absorption versus concentration from the molar absorptivity determination for the basic and singly protonated forms of one of the compounds (**7**) are provided in the Supporting Information, Figures S.15–S.19, along with a discussion of the procedures used to obtain the data.

Molar absorptivities for the nonprotonated forms of compounds **1–3** were also determined in DMSO and 50% EtOH/H_2O, and molar absorptivities of the singly protonated forms of compounds **1–3** were determined using HCl as the protonating acid for studies carried out in DMSO and using $HClO_4$ as the protonating acid for studies carried out in 50% EtOH/H_2O. All of the aforementioned absorptivities were determined in duplicate by linear regression, and the ideal concentrations of acid used to determine absorptivities of the singly protonated forms were

determined from the protonation studies mentioned previously. Molar absorptivities of the singly protonated forms of **1–3** using $HClO_4$ in ACN were also estimated by single point measurements (rather than linear regression). These measurements were also carried out at least twice. Linear regression determination of absorptivity using perchloric acid in ACN was not possible when the acid concentration was held constant, as the equilibrium was perturbed too greatly when the concentration of dye was changed; it is unknown why this behavior was only observed for $HClO_4$ and not for HCl (although it may be related to the acid strength).

Correlated NMR-absorption studies. Derivative **1** was selected for the correlated NMR-absorption studies because of simplicity of spectral interpretation and the presumption that, given its phenyl substitution, its behavior is representative of most of the compounds studied. Solutions containing 0.5 m*M* of compound **1** were utilized to facilitate the measurement of both the absorption and NMR spectra of each sample, and absorptivities were measured using a reduced pathlength (0.2 cm) cuvette. Unfortunately, for these samples, some of the measured absorption values were too high for quantitative measurement ($A > 2$), but as no detector saturation was observed, the measurements were still usable for qualitative determination of the species present in a given sample.

An initial protonation study was carried out in which a 0.5-m*M* solution of compound **1** was protonated with varying concentrations of $HClO_4$ in ACN, and the concentrations of acid corresponding to the first and second protonation equilibria were determined. Using this information, six samples were prepared, each containing 0.5 m*M* of compound **1** and varied concentrations of $HClO_4$. Concentrations of acid were chosen that corresponded to both the first and second equilibria, including one sample containing no added acid, one sample containing a concentration of acid corresponding to the maximum concentration of the singly protonated form of **1**, one sample containing a concentration of acid corresponding to all of compound **1** being in the doubly protonated form, and the rest of the samples containing intermediate acid concentrations in which two species are present. NMR and absorption spectra of each sample were acquired simultaneously at 25°C over the course of a single evening. Additional NMR studies were carried out at higher (37°C) and lower (0°C) temperatures to ensure that the observed behavior was not temperature dependent. These higher and lower temperature studies were carried out without the associated absorption measurements as no thermostatted UV-visible spectrophotometers were available; however, the color changes and intensities were noted visually.

Spectroscopic pK_a determination. As the donor strength of the substituents at the 2 and 6 positions was found to have a marked effect on the molar absorptivities of the intermediate singly protonated species, three dyes were chosen for further study of this substitution effect. Compounds **1–3** were chosen on the basis of a decreasing scale of electron-donating tendencies; derivative **2** possessed *p*-tolyl substituents (most electron-donating) at the 2 and 6 positions; derivative **1** possessed "intermediate" phenyl substitution, and derivative **3** possessed *p*-chlorophenyl substitution (least electron-donating).

The acid dissociation constants p_sK_{a1} and p_sK_{a2} of compounds **1–3** were determined spectroscopically in 50% EtOH-H_2O. This solvent system was chosen to allow direct pH measurement with a standard pH electrode. Solutions contained 20 μM dye and increasing concentrations of $HClO_4$ to vary the pH. Ionic strengths of each sample were adjusted to 0.1*M* using NaCl, and appropriate volumes of EtOH and deionized H_2O were added such that the final solvent composition was 50% EtOH/H_2O (*v*/*v*). It should be noted that ionic strengths were adjusted to a constant value as preliminary studies carried out on two of the compounds indicated that large changes in ionic strength are capable of perturbing the protonation equilibrium to some extent. Each solution was thoroughly mixed, and then part of the solution was transferred into a cuvette for measurement of the absorption spectrum. A pH electrode was inserted into the remaining solution, and the pH was measured at the same time as the absorption spectrum.

The p_sK_a values of these compounds were determined plotting the absorption at the red-shifted ICT wavelength corresponding to the singly protonated species ($A_{\lambda,\ HB+}$) as a function of pH and solving for the pK_a. As the absorption at this wavelength is zero when no acid is present (all dye is in the basic form) and goes to zero when sufficiently high concentrations of acid are present (all dye is in the doubly protonated form H_2B^{2+}), any absorption at this wavelength is presumably proportional to the concentration of the singly protonated species HB^+ (C_{HB+}) as per Beer's law ($A_{\lambda,\ HB+} = \varepsilon b C_{HB+}$). Plotting absorption at λ_{HB+} as a function of pH results in a curve with a maximum absorption $A_{\lambda,\ HB+\ MAX}$ at the pH corresponding to the maximum concentration of the singly protonated species. Accordingly, both p_sK_a values were determined by plotting absorption at $\lambda_{\ HB+}$ as a function of pH, determining $A_{\lambda,\ HB+\ MAX}$, and solving for pH for $A_{\lambda,\ HB+} = ½\ A_{\lambda,\ HB+\ MAX}$ at pH lower than the pH corresponding to $A_{\lambda,\ HB+\ MAX}$ (to determine p_sK_{a1}) and at pH higher than the pH corresponding to $A_{\lambda,\ HB+\ MAX}$ (to determine p_sK_{a2}).

Acknowledgments. This work is supported by the GSU Research Initiation Grant and Georgia Research Alliance Grant to MH. Additionally, the authors would like to acknowledge the Center for Diagnostics and Therapeutics at Georgia State University for their support. The funding agencies had no involvement in the design, collection, analysis, or interpretation of data, the writing of this report, or the decision to submit this article for publication. The authors would also like to acknowledge Drs Alex Spring, Sekar Chandrasekaran, and Markus Germann for their assistance with the NMR spectrometers.

DISCLOSURE

This manuscript has been read and approved by all authors. This article is unique, is not under consideration by any other publication, and has not been published elsewhere. The authors and peer reviewers of this article report no conflicts of interest. The authors confirm that they have permission to reproduce any copyrighted material.

REFERENCES AND NOTES

[1] Hisamatsu, N.; Hiraishi, S. Thermal recording material providing yellow image. Japanese Patent 10250237, September 22, 1998.

[2] Grasshoff, J. M.; Marshall, J. L.; Minns, R. A.; Ramos, S. M.; Stroud, S. G.; Telfer, S. J.; Yang, H.; Boggs, R. A.; Kolb, E. S. Process and composition for generating acid for imaging compositions. International Patent 9824000, June 4, 1998.

[3] Angadiyavar, C. S.; Srinivasan, R. 2,4,6-Trisubstituted pyridine dye lasers. U.S. Patent 506916, February 3, 1976.

[4] Tang, B.; Yu, F.; Li, P.; Tong, L.; Duan, X.; Xie, T.; Wang, X. J. Am. Chem. Soc. 2009, 131, 3016.

[5] Garcia-Acosta, B.; Martinez-Manez, R. Sancenon, F.; Soto, J.; Rurack, K.; Spieles, M.; Garcia-Breijo, E.; Gil, L. Inorg. Chem. 2007, 46, 3123.

[6] Reichardt, C. Solvents and Solvent Effects in Organic Chemistry. VCH Verlagsgesellschaft mbH, Weinheim, Germany, 1988, p. 287.

[7] Nishiyama, S.; Tajima, M.; Yoshida, Y. Mol. Cryst. Liq. Cryst. 2007, 472, 33[423].

[8] Adib, M.; Mohamadi, A.; Sheikhi, E.; Ansari, S.; Bijanzadeh, H. R. Synlett 2010, 11, 1606.

[9] Franke, A.; Mueller, J.; Lietz, H.; Wiersdorff, W. W.; Hege, H. G.; Mueller, C. D.; Gries, J.; Lenke, D.; Von Philipsborn, G.; Raschack, M. Aminopropanol derivatives of 2-hydroxy-β-phenylpropiophenones, pharmaceutical compositions and use. U.S. Patent 4540697, September 10, 1985.

[10] Petrik, G. Aminopropanol derivatives of 2-hydroxy-β-phenylpropiophenones and a pharmaceutical agent containing them. German Patent 3328376, January 32, 1985.

[11] Franke, A.; Mueller, J.; Lietz, H.; Wiersdorff, W. W.; Hege, H. G.; Mueller, C. D.; Gries, J.; Lenke, D.; Von Philipsborn, G.; Raschack, M. Aminopropanol derivatives of 2-hydroxy-β-phenyl propiophenones and therapeutic agents containing them. European Patent 75207, March 30, 1983.

[12] Raghukumar, V.; Thirumalai, D.; Ramakrishnan, V. T.; Karunakara, V.; Ramamurthy, P. Tetrahedron 2003, 59(21), 3761.

[13] Zhao, B.; Lu, W.-Q.; Zhou, Z.-H.; Wu, Y. J. Mater. Chem. 2000, 10(7), 1513.

[14] Aldag, R.; Neumann, P.; Boettcher, A.; Bluemel, T.; Seitz, F.; Raulfs, F. W. Photopolymerizable materials for photoresists and lithographic plates. European Patent 291880, November 23, 1988.

[15] Usami, T. Heat-sensitive nonimpact printing sheets. Japanese Patent 62113588, May 25, 1987.

[16] Sano, M.; Iwakura, K. Image recording materials. Japanese Patent 61233580, October 17, 1986.

[17] Joule, J. A.; Mills, K. Heterocyclic Chemistry; John Wiley & Sons Ltd.: West Sussex, 2010.

[18] Huber, W. Titrations in Nonaqueous Solvents; Academic Press, Inc.: New York, 1967.

[19] Eckert, F.; Leito, I.; Kaljurand, I.; Kütt, A.; Klamt, A.; Diedenhofen, M. J. Comp. Chem. 2009, 30(5), 799.

[20] Fritz, J. S. Acid Base Titrations in Nonaqueous Solvents; Allyn & Bacon Inc.: Boston, 1973.

[21] Mujumdar, R.; Smith, J. A. pH-Sensitive cyanine dyes as reactive fluorescent reagents. European Patent 1394219, March 3, 2002.